

A CORRELATION STUDY BETWEEN INTERGRANULAR STRAINS AND MAGNETIC PROPERTIES OF MILD STEEL

R. Hutanu¹, L. Clapham¹, and R. Rogge²

¹Department of Physics, Stirling Hall, Queen's University, Kingston, Ontario, Canada; ²National Research Council Canada, Neutron program for Materials Research, Chalk River Laboratories, Chalk River, Ontario, Canada

Abstract: Residual stresses appear due to non-uniform plastic deformation that occurs, for example, during the manufacture of engineering materials. The importance of a complete understanding of the residual stress mechanisms is vital since they add to the external applied stresses leading to unexpected failures. The microscopic residual stresses are caused by the complex grain-grain interaction in a deformed polycrystalline material. These residual stresses, which are named intergranular residual stresses (IS) were found, using neutron diffraction, to be large along the $\langle 100 \rangle$ crystallographic directions [1-4]. Interestingly, $\langle 100 \rangle$ is the magnetic easy axis in steels as determined by the Magnetic Barkhausen Noise (MBN) method. Our work focuses on finding the correlation between the IS and magnetic behaviour of steels based on MBN, neutron diffraction and stress relief experimental data. Several mild steel samples were deformed at different plastic deformation levels then unloaded. We have found that the magnetic easy axis detected in these samples is strongly related to the $\langle 100 \rangle$ IS.

Introduction: Residual stresses are present in a material after the plastic deformation of this material followed by unloading. In the presence of residual stresses, materials will yield plastically at a lower applied stress than a specimen free of residual stresses and thus, the resistance to fracture will be affected. There are mainly two types of residual stresses: Type 1 stresses which are the macroscopic residual stresses appearing on the length scale of the sample and the recently recognized Type 2 intergranular residual stresses (IS) which develop on the scale of the grain size.

Residual stress formation. Type 1 residual stresses are present in a polycrystalline sample to preserve the stress continuity over the entire sample. Residual stresses are elastic in nature and the net force along any cut plane must be equal to zero [5]. In the case of elastic IS, the phenomenology is similar, but on a smaller scale, with IS maintaining the stress compatibility among the grains in the same manner as Type 1 stresses do for the macroscopic sample.

The evolution of IS can be illustrated by the case of uniaxial load of a polycrystalline sample. During the first elastic deformation stage, the applied load will be non-uniformly distributed among the grains in different crystallographic orientations due to the fact that the polycrystalline sample is elastically anisotropic. As the deformation increases towards the plastic regime, the grains that are elastically stiff (with high elastic moduli) in the tensile direction will yield before other grains. Further deformation results in the unyielded grains accumulating intergranular strains transferred from the plastically deformed grains. The result, after unloading, is that strain is non-uniformly distributed between crystallographic directions. Neutron diffraction studies showed that this is the case for most bcc and fcc steels, where after deformation + unloading the $\langle 100 \rangle$ directions have very high IS values compared to other crystallographic directions [1-4]. As mentioned previously, these results have interesting magnetic implications since the easy magnetization direction in steels lies along the $\langle 100 \rangle$ crystallographic directions.

It is well known in the literature that low temperature annealing (400-500°C) is associated with recovery processes in steels [9,10]. These recovery processes lead to the relieving of residual stresses, although the temperatures are not sufficiently high to produce recrystallization. In this study, this annealing method was employed in order to study the relief of IS.

Magnetic Barkhausen Noise (MBN): MBN occurs when a ferromagnetic material such as steel is subjected to a changing magnetic field. The technique based on MBN has been used as a nondestructive experimental tool for the detection of residual stresses in ferromagnetic samples. Ferromagnetic materials are composed from magnetic domains, each domain being defined by a magnetization vector which is the sum of all the atomic magnetic moments within that domain. This division into magnetic domains takes place due to minimum energy principle and this same principle dictates the alignment of the magnetization vector of a domain along the $\langle 100 \rangle$ direction in iron. These directions are called the easy magnetization directions. A bulk easy magnetization axis occurs in a polycrystalline sample if the individual easy axes from different grains align preferentially along a particular sample direction.

A domain wall is defined by the layer that exists between two magnetic domains. In the presence of an external magnetic field, the magnetic domains configuration changes in order to lower the total energy. Domain walls move as domain magnetization vectors try to align with the externally applied field, with favourably oriented domains

growing at the expense of less favourable ones. Domain wall movement is not continuous, however, since walls must overcome local pinning sites such as grain boundaries or impurities. The MBN effect is associated with the abrupt irreversible movements of the domain walls when unpinning occurs, and the MBN signal is highest in the direction of the bulk magnetic easy axis [6].

If a tensile stress is applied to the ferromagnetic material, the energetically favourable magnetic domains will reorient and expand in the $\langle 100 \rangle$ directions closest to the stress axis. As a result, the bulk magnetic easy axis will shift towards the tensile axis [7]. The MBN signal will increase in the direction of applied tensile stress [7,8]; conversely, it will decrease in the direction of the applied compressive stress [7,8]. Residual stresses have the same effect on the MBN signal as the active applied stresses [9].

Figure 1 is a schematic diagram of the apparatus used for MBN generation and detection. The waveform generator and power supply provide a low frequency (12 Hz) alternating current to a coil wrapped around a U-shaped core as shown. This magnetizes the sample sitting below. A pick-up coil or read head between the magnetic poles detects the high-frequency Barkhausen noise pulses, which are amplified, filtered, displayed and analysed in a LabView environment. The parameter that we commonly use for the MBN analysis is the MBN_{energy} which is obtained by integrating the square of the induced voltage with respect to time.

In order to detect the existence of the bulk magnetic easy axis in the sample, an angular MBN set-up is used. In this angular configuration, the exciter magnet together with the pick-up coil is rotated every $\theta = 10^\circ$ around a fixed axis on the sample surface. The result is displayed on a polar plot of MBN_{energy} vs angle θ and the data is fitted with the following equation [11]:

$$MBN_{energy} = \alpha \cos^2(\theta - \phi) + \beta \quad (1)$$

where α is a parameter associated with the proportion of 180° domains that contribute to the easy axis, θ is the angle of the applied magnetic field with the direction of the easy axis. Angle ϕ defines the direction of the easy axis and β is related to the isotropically oriented 180° domains that form the background noise of the MBN signal. The bulk magnetic easy axis of the sample will be then indicated by an elongation of the polar plot in a particular direction.

In addition to the angular measurements, linear MBN experiments can be conducted with a different set-up in order to check for residual stresses variations along the samples length. The MBN linear scanner is of similar design to the apparatus shown in Figure 1. In addition, this set-up includes a pneumatic valve system to apply a consistent pressure to the MBN probe, and stepper motors for accurate positioning of the detection tool (read-head) on the sample. Both are computer controlled using LabView.

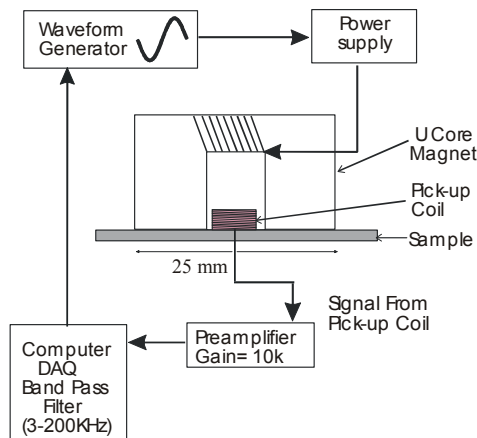


Figure 1. Diagram of the MBN apparatus.

Neutron diffraction: Using neutron diffraction as an experimental tool to map strains has a lot of advantages. Neutrons are highly penetrating, they are non-destructive and no sample preparation is needed.

In-depth stress mapping can be performed using neutron diffraction technique, thus providing valuable information for the understanding of the residual stress influence on MBN. Neutron diffraction phenomenon is governed by Bragg's law:

$$\lambda = 2d_{hkl} \sin \theta_{hkl} \quad (2)$$

where λ is the neutron beam wavelength, d_{hkl} is the lattice spacing for an (hkl) plane and $2\theta_{hkl}$ is the diffraction angle. If the sample is plastically deformed, after unloading, residual strains will be present within the sample volume. The residual strain ε_{hkl} , of the lattice for a particular direction <hkl> can be then computed from the following equation:

$$\varepsilon_{hkl} = \frac{d_{hkl} - d_0}{d_0} \quad (3)$$

with d_0 being the stress-free lattice spacing that is obtained from an un-deformed sample. Neutron diffraction is ideal for measuring IS in samples because within a given sample the strains for each particular <hkl> direction can be isolated and measured.

Neutron diffraction measurements were carried out on the E3 spectrometer at the NRU, Chalk River, Canada. The (115) plane of a Ge monochromator crystal was used to produce neutron beams of $\lambda = 1.539 \text{ \AA}$ wavelength. The residual strains for each of the deformed samples were measured separately for three different crystallographic reflections: {211}, {220} and {200}. The sample co-ordinate system was described as follows: the applied stress axis was parallel to the rolling direction (RD) of the initial plate from which the samples were cut. The direction perpendicular to the RD in the sample plane was named the transverse direction (TD) while the direction normal to the sample plane was termed the normal direction (ND). The data was obtained for different angular orientations in the ND-RD-TD plane. For this angular set-up, the samples were EDM cut in squares of $1 \times 1 \text{ cm}^2$ then stacked together. The diffracted peaks were obtained using a multiple (32 wire) detector spanning an angle of $\sim 2.5^\circ$. The scattering angle $2\theta_{hkl}$ of the peak for a certain reflection {hkl} was determined by fitting the experimental profile of counts versus angular position to a Gaussian peak shape on a sloping background. The angle θ_{hkl} was then used in equation (2) to determine the value of d_{hkl} and the value of the residual strains was calculated using equation (3).

The Elasto-Plastic Self-Consistent (EPSC) model: The results of the neutron diffraction strain measurements were compared with the Elasto-Plastic Self-Consistent (EPSC) model. This model, developed by Turner and Tome [12], provides a numerical code to predict the elastic and plastic behavior of each grain within the deformed polycrystalline aggregate. In this theory, the individual grains are characterized by their orientations relative to the sample's coordinate system (rolling, transverse and normal directions - RD, TD, ND respectively) and by 'weights' which account for the volume fractions estimated by the texture data. In addition, each grain is considered to be an ellipsoidal inclusion in a homogeneous effective medium (HEM) which gives the overall response of the sample. The fundamental interaction equation between grains and HEM is given by:

$$(\sigma - \Sigma) = -L : (S^{-1} - I) : (\varepsilon - \mathcal{E}) \quad (4)$$

where σ and ε are the grain stress and strain rates tensors while Σ and \mathcal{E} are the HEM overall stress and strains rates tensors. L is the overall elasto-plastic stiffness tensor describing the mechanical parameters of the HEM and S is the Eshelby tensor which is a function of L and the shape of the inclusion. The boundary condition requires that either Σ or \mathcal{E} is specified.

The input parameters of the code are the elastic constants and the plastic deformation parameters of the sample, the number of diffraction directions and the initial crystallographic texture of the sample. The code calculates the strain of each grain subset (characterized by grains in the same orientation) incrementally as the process of loading or unloading evolves. The amount of residual strains in any selected direction is determined at the end of the unloading process.

Results: The procedure to examine the correlation between intergranular strain (IS) and magnetic behavior in steels can be summarized as follows:

1. MBN and neutron diffraction studies of IS were conducted on mild steel samples before and after deformation. At low strain (1%), the sample exhibited shear banding, and measurements were made in banded and band-free regions.
2. Samples were heat treated to 'stress relieving' temperatures, with MBN and neutron diffraction measurements performed before and after annealing.

Samples and experiments: Several tensile mild steel samples with dimensions (in the central region) of $155 \times 30 \times 3 \text{ mm}^3$ were plastically deformed to strain levels of 1%, 3%, 5%, 10% and 20% followed by unloading. However, only the data for the samples deformed at 1% and 10% samples will be shown in this work. Luders bands [13] formed during the earliest stages of plastic deformation (1%) and, as the amount of deformation increased, the bands propagated until the entire sample's surface was deformed. Thus, the Luders bands were the 'carriers' of the plastic deformation. The sample deformed at 1% was inhomogeneous along its length, exhibiting regions with Luders bands and regions without. The samples deformed in the strain range 3%-20% were homogeneous.

Experimental data: 3.2.1 MBN results after deformation: The linear and the angular MBN data for the sample deformed at 1% strain followed by unloading is shown in Figure 2 below. The high MBN_{energy} signal from Figure 2(a) was detected in Luders bands region of the sample, indicating a higher level of residual stresses. Figure 2(b) shows the results of angular measurements, both before deformation and in the Luders bands region after deformation in the 1% strain sample. As seen here, no magnetic easy axis was detected before deformation. The unbanded region of the deformed sample displayed an identical result to that of the undeformed sample. However, the banded region was characterized by a significant bulk magnetic easy axis in the TD direction indicating the presence of tensile residual strain in this direction. The samples deformed between 3% and 20% strain levels had a uniform MBN level along their length, as shown by Figure 3(a) in the case of the 10% sample, and no distinct banded/unbanded regions. Angular MBN measurements revealed, for all these samples, a distinctive TD magnetic easy axis, as in case of the 10% sample (Figure 3(b)).

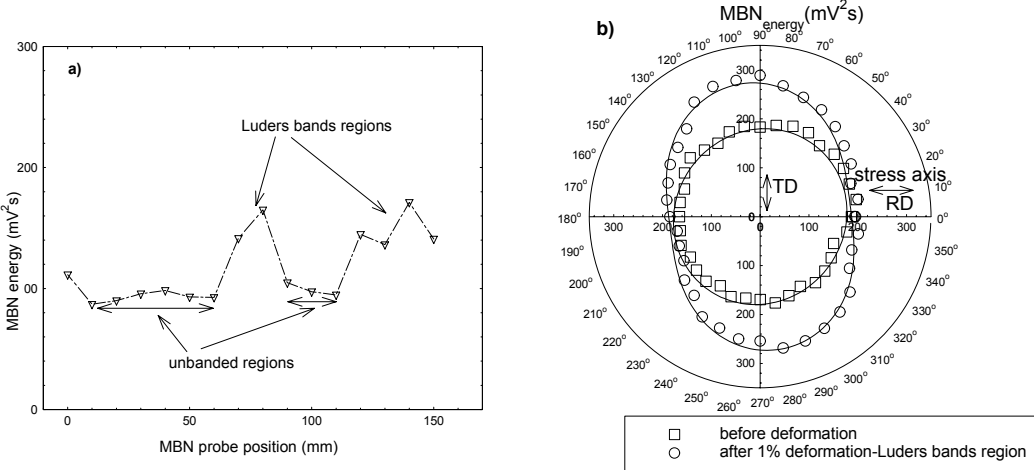


Figure 2. MBN linear data (a) and MBN angular data (b) for the Luders bands region of the sample deformed at 1% plastic strain followed by unloading. The direction of the original stress axis (before unloading) is indicated on the angular plot.

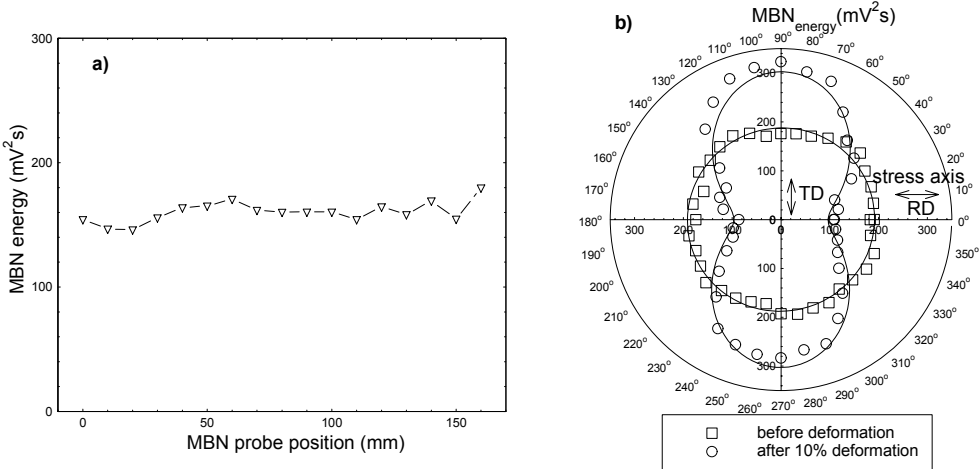


Figure 3. MBN linear data (a) and MBN angular data (b) for the sample deformed at 10% strain.

3.2.2 Neutron diffraction data and the EPSC model: The results of the EPSC model together with the neutron diffraction data for the sample deformed at 1% strain (banded region) are shown in Figure 4 for the {200}, {211} and {220} reflections. Similar trends are seen for the 10% sample, data that is not shown here. As it can be observed from Figure 4, the experimental data agrees well with the model, similar results also obtained for the rest of the deformed samples.

Since the magnetic easy axis lies in the $\langle 100 \rangle$ crystallographic directions in steel, we may expect to see a correlation between the MBN results and the $\langle 200 \rangle$ strains (note the strain in the $\langle 200 \rangle$ and $\langle 100 \rangle$ are identical). The results of Figure 4(a) show a fairly complex variation of $\langle 100 \rangle$ residual strain. Although the effect of this variation on MBN is not yet fully understood, on a qualitative level Figure 4(a) indicates a high $\langle 100 \rangle$ strain in the TD and a lower $\langle 100 \rangle$ strain in the RD – this is consistent with the directions of highest and

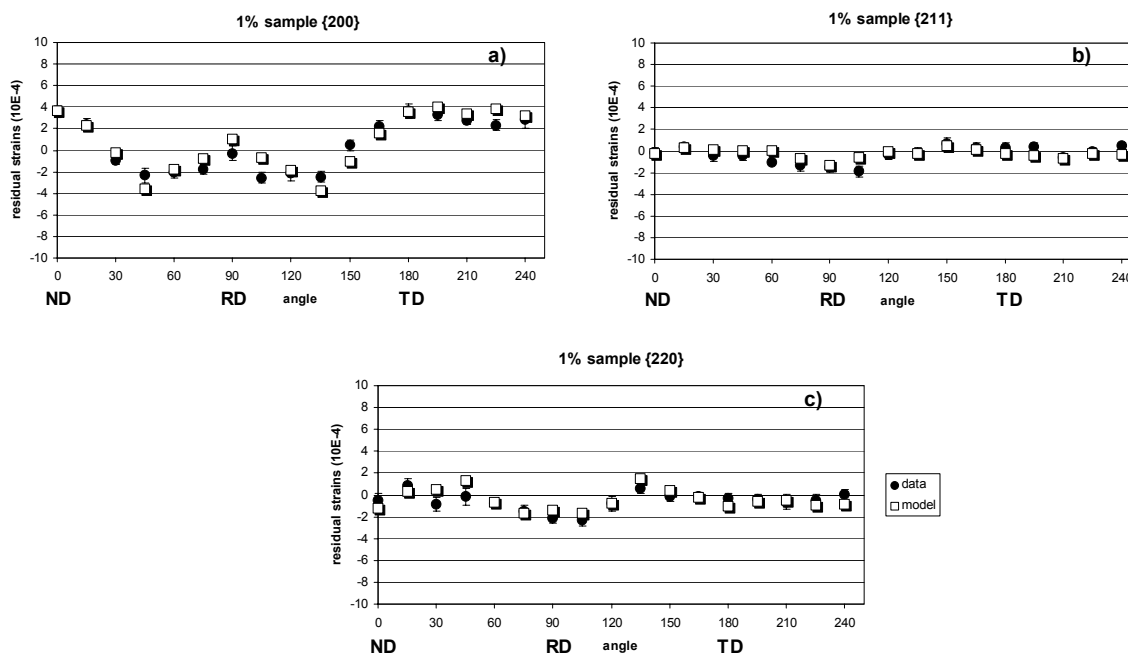


Figure 4. Neutron diffraction data and the EPSC simulations results for the 1% sample for a) {200}, b) {211} and c) {220} reflections.

lowest MBN signal seen in Figure 2(b). At the same time, the {211} residual strains (Figure 4(b)), which are the macroscopic strains, are insignificant for the directions within the TD-ND plane. This important result implies that for the transverse direction (TD), which is the direction of detected magnetic easy axis, there are mainly intergranular residual strains along the $\langle 100 \rangle$ directions. In addition, as shown by Figure 4(c), the {220} strains are negligible for the TD direction.

Comparison of MBN and neutron diffraction results after annealing: In order to observe the intergranular residual strain relief process, the deformed samples were annealed at temperatures between 400 and 600°C. Figure 5 shows the IS relief of the 1% sample (banded region) after annealing at 500°C for 30 minutes. Subsequent annealing of the same sample for longer periods of time didn't show a significant effect, as detected by MBN.

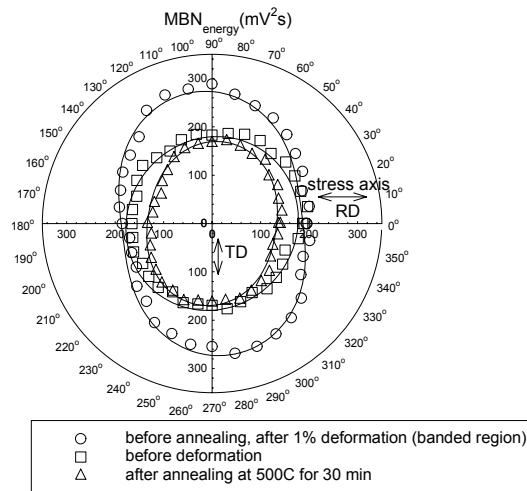


Figure 5. MBN angular data after annealing for the sample deformed at 1% strain (banded region).

Neutron diffraction measurements were taken after the final annealing (550°C) and the results for the same sample (1%) are shown in Figure 6. The largest annealing effect detected by neutron diffraction was for the {200} tensile residual strains in the TD-ND plane. This result is in agreement with the large tensile residual stresses relief along the TD direction exhibited by the angular MBN data.

Discussion: The results of this study showed that the 1% plastic deformation created a magnetic easy axis in the TD direction ($\langle 100 \rangle$), perpendicular to the tensile axis, for the banded region of the sample. The neutron diffraction results showed that for the same TD direction the $\langle 200 \rangle$ IS were very high, although the residual strain in the other two measured directions $\langle 211 \rangle$ and $\langle 220 \rangle$ was near zero.

A magnetic easy axis could also be caused by a $\langle 100 \rangle$ deformation texture. This is unlikely, however, since the post-annealed MBN data indicated little or easy axis, and annealing at this temperature would not have altered the sample texture. In addition, the neutron diffraction texture data showed that the $\langle 100 \rangle$ deformation texture is very weak. Thus we conclude that there is a significant correlation between the magnetic easy axis detected by angular MBN and the IS strains in the $\langle 200 \rangle$ direction. Similar results were found for the rest of the deformed samples. The dependence of the MBN_{energy} on the $\langle 200 \rangle$ IS strains is approximately linear and is shown in Figure 7 for 1% and 10% samples together with the linear fits. The MBN data for this plot was obtained from the MBN angular plots at 30°, 60° and 90° angles within the RD-TD plane. Linear fits were also obtained for the rest of the samples (3%, 5% and 20% strain). It is interesting to note that the slopes of the linear fits in Figure 7 increase with the overall deformation level. This suggests that the MBN signal is being affected also by other factors; perhaps

plastic deformation or texture. This is the subject of continuing work.

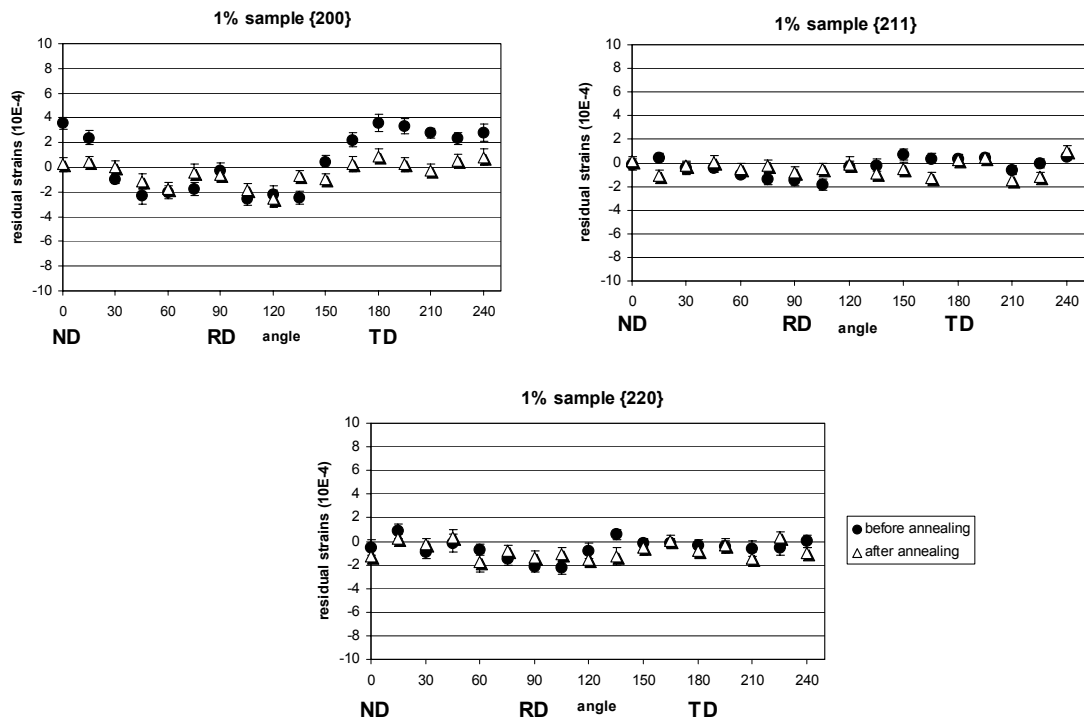


Figure 6. Neutron diffraction data before and after annealing for the 1% sample (banded region).

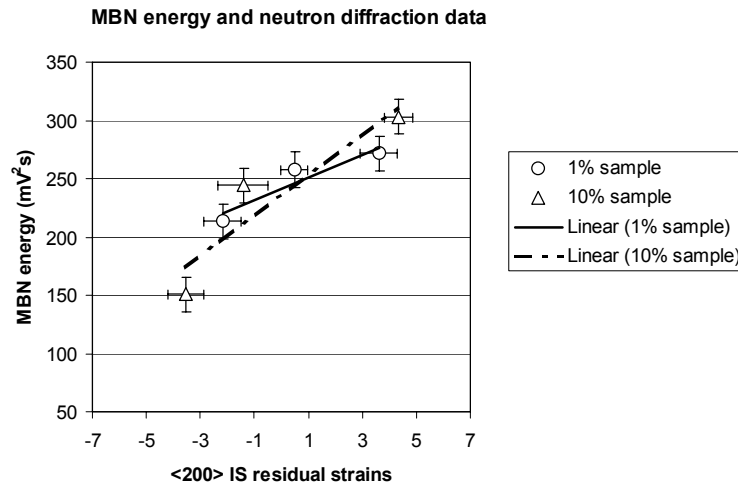


Figure 7. Linear dependence of the MBN_{energy} versus $\langle 200 \rangle$ residual strains for the 1% and 10% samples.

Conclusions: In order to study the correlation between the magnetic easy axis and intergranular residual strains in steels, five mild steel samples were plastically deformed and then unloaded. The 1% sample exhibited both Luders bands regions as well as unbanded regions. The rest of the samples (3%-20%) were homogeneously deformed, as the Luders bands covered their entire surfaces. A magnetic easy axis was detected for all the samples; this axis was found to be strongly correlated to the $\langle 200 \rangle$ IS. A linear dependence between the MBN_{energy} and the IS was obtained. In addition, the experimental neutron diffraction results agreed well with the EPSC model predicted data.

References:

1. Pang J.W.L., Holden T.M., Wright J.S., Mason T.E., *Acta Mater.*, **48**, 1131-1140 (2000).
2. Pang J.W.L., Holden T.M., Mason T.E., *J. Strain Analysis*, **33**, 373-383 (1998).
3. Pang J.W.L., Holden T.M., Mason T.E., *Acta Mater.*, **46**, 1503-1518 (1998).
4. Holden T.M., Clarke A.P., Holt R.A., *Metall. Mater. Trans. A*, **28**, 2565-2576 (1997).
5. Dieter G. E., *Mechanical Metallurgy*, McGraw-Hill, New York, 1961.
6. Krause W. T., Szpunar J.A., Birsan M., Atherton D.L., *J. Appl. Phys.*, **79**, 3156-3167(1996).
7. Krause W. T., Clapham L., Pattantyus A., Atherton D. L., *J. Appl. Phys.*, **79**, 4242-4252 (1996).
8. Krause W. T., Makar J. M., Atherton D. L., *J. Mag. Mag. Mater.*, **137**, 25-34 (1994).
9. Clapham L., Heald C., Krause T., Atherton D. L., *J. Appl. Phys.*, **86**, 1574-1580 (1999).
10. Rahim T., 'The effect of plastic deformation and residual stress on Magnetic Barkhausen Noise and Magnetic Flux Leakage signals for mild steel', MSc thesis, Queen's University, 2003.
11. Krause W.T., Clapham L., Atherton D.L., *J. Appl. Phys.* **75**, 7983-7988 (1994).
12. Turner P.A. and Tome C. N., *Acta Metall. Mater.*, **42**, 4143-4153 (1994).
13. Hall E. O., *Yield Point Phenomena in Metals and Alloys*, Plenum Press, New York, 1970.